Published in final edited form as:
J Mol Biol. 2008 August 1; 381(1): 102–115. doi:10.1016/j.jmb.2008.05.062.

Effect of Flap Mutations on Structure of HIV-1 Protease and Inhibition by Saquinavir and Darunavir

Fengling Liu[1,#], **Andrey Y. Kovalevsky**[1,*], **Yunfeng Tie**[1], **Arun K Ghosh**[3], **Robert W. Harrison**[4,1], and **Irene T. Weber**[1,2]

[1] Department of Biology, Molecular Basis of Disease Program, Georgia State University, Atlanta, GA 30303, USA

[2] Department of Chemistry, Molecular Basis of Disease Program, Georgia State University, Atlanta, GA 30303, USA

[3] Department of Chemistry and Medicinal Chemistry, Purdue University, West Lafayette, IN 47907, USA

[4] Department of Computer Science, Molecular Basis of Disease Program, Georgia State University, Atlanta, GA 30303, USA

Abstract

HIV-1 protease (PR) and its mutants are important antiviral drug targets. The PR flap region is critical for binding substrates or inhibitors and catalytic activity. Hence, mutations of flap residues frequently contribute to reduced susceptibility to PR inhibitors in drug resistant HIV. Structural and kinetic analyses were used to investigate the role of flap residues Gly48, Ile50 and Ile54 in the development of drug resistance. The crystal structures of flap mutants PR_{I50V}, PR_{I54V}, and PR_{I54M} complexed with saquinavir (SQV) and PR_{G48V}, PR_{I54V}, and PR_{I54M} complexed with darunavir (DRV) were determined at the resolutions of 1.05–1.40 Å. The PR mutants showed changes in flap conformation, interactions with adjacent residues, inhibitor binding and the conformation of the 80's loop relative to the wild type PR. The PR contacts with darunavir were closer in PR_{G48V}-DRV than in the wild type PR-DRV, while they were longer in PR_{I54M}-DRV. The relative inhibition of PRs with mutations I54V and I54M was similar for saquinavir and darunavir. PR_{G48V} was about 2-fold less susceptible to saquinavir than to darunavir, while the opposite was observed for PR_{I50V}. The observed inhibition was in agreement with the association of G48V and I50V with clinical resistance to saquinavir and darunavir, respectively. This analysis of structural and kinetic effects of the mutants will assist in development of more effective inhibitors for drug resistant HIV.

Keywords

drug resistance; aspartic protease; saquinavir; darunavir (TMC114)

*Corresponding author: Irene T. Weber, Department of Biology, Georgia State University, P.O. Box 4010, Atlanta, GA 30302-4010, USA, Phone 404 413-5411, FAX 404 413-5301, iweber@gsu.edu.
[#]current address: Department of Structural Biology, Stanford University School of Medicine, Stanford CA 94305.
[*]current address: Bioscience Division, MS M888, Los Alamos National Laboratory, Los Alamos NM 87545.

INTRODUCTION

HIV-1 (Human immunodeficiency virus type 1) protease (PR) is an effective drug target for antiviral inhibitors. Each subunit of the active PR homodimer has a glycine-rich region termed the flap comprising residues Lys[45]-Met-Ile-Gly-Gly-Ile-Gly-Gly-Phe-Ile-Lys[55], which fold into two anti-parallel β strands. The flexible flaps participate in the binding of a substrate or inhibitor in the active site cavity of PR [1; 2; 3]. The importance of residues in the flap for PR activity has been characterized through large scale mutagenesis [4]. The residues Met46, Phe53 and Lys55 are the most tolerant of substitutions; Ile47, Ile50, Ile54 and Val56 only tolerate a few conservative substitutions; and Gly48, Gly49, Gly51, Gly52 are the most sensitive to mutation. Therefore, mutations in the flap residues may alter the enzyme activity, conformation and flexibility of the flap. Mutations in flap residues 46, 47, 48, 50, 53, and 54 are frequently observed in drug resistant mutants of HIV and show various levels of reduced drug susceptibility to different PR inhibitors (PIs) [5; 6]. Altered flap conformations have been reported for protease and its mutants in the unliganded form [7; 8; 9] or with bound peptide [10]. Previously, we have analyzed the structures, activities, inhibition and stability of PR variants with the single substitutions of flap residues M46L, G48V, I50V, and F53L [8; 11; 12; 13; 14; 15]. These studies use PR from HIV-1 subtype B, which forms about 10% of global infections with HIV-1 group M compared to ~50% for subtype C [16]. Recently, the PRs from subtype C and F were analyzed [17; 18]. These subtypes contain 8–10 polymorphic substitutions in the sequence outside of the flaps and inhibitor binding site, which can influence catalytic activity and inhibition. The PR structures and interactions with inhibitors were very similar to those of the B subtype PR, with larger structural variations in surface residues 34–42 for the F subtype PR and 65–69 for the C subtype PR.

Saquinavir (SQV) was the first PR inhibitor to be approved by the FDA in 1995, and is still widely used in AIDS therapy, along with nine other inhibitors. The latest, darunavir (DRV, previously known as TMC114), a chemical derivative of the PR inhibitor amprenavir, was approved in 2006 for salvage therapy and is extremely potent against the wild type PR and most drug resistant mutants *in vitro* and *in vivo* [11; 19; 20; 21]. Darunavir, boosted with ritonavir, is recommended for treatment-experienced patients who respond poorly to other PIs. Saquinavir was designed to target the wild type PR and its chemical structure contains a number of peptidic main chain groups mimicking a natural substrate of PR as shown in Figure 1a[22]. In contrast, darunavir was designed to be less peptidic while introducing more hydrogen bond interactions with the main chain atoms of PR in order to maintain its effectiveness on PR variants [20; 23].

In this study, PR variants with the individual flap mutations G48V, I50V, I54V and I54M were analyzed to gain insight into their role in the development of drug resistance. G48V is one of the primary drug resistant mutations selected during treatment with saquinavir [24; 25]. I50V arises in treatment with amprenavir, and also confers resistance to darunavir [5]. Mutations of I54M and I54V are commonly observed during therapy with multiple PR inhibitors [5; 26; 27; 28]. Several mutations of Ile54 are present in isolates with reduced susceptibility to saquinavir. Mutations I54M and I54L are frequent in clinical isolates resistant to darunavir [29]. Moreover, Met was the most frequently identified substitution of residue 54 after treatment with amprenavir, which is chemically related to darunavir [28]. Residue 50 lies at the tip of the PR flap, while residues 48 and 54 are located on opposite β strands of the flap (Figure 1b). Previously, the crystal structure of the double mutant G48V/L90M with saquinavir was analyzed [30], and we reported the structure of the PR_{I50V} mutant with darunavir [11]. Here, the crystal structures of flap mutants PR_{G48V}, PR_{I50V}, PR_{I54V}, and PR_{I54M} were solved in complexes with saquinavir and darunavir. Comparison of the mutant and wild type structures revealed changes in the flap conformation, interactions between flap residues from the two PR subunits, inhibitor binding and conformation of residues 78–82 (the 80's loop). The kinetic

data are discussed in relation to the structural changes. This analysis confirmed the important roles of residues in the flaps and enhanced our understanding of the drug resistant mechanisms used by the flap mutants.

RESULTS AND DISCUSSION

Kinetics

The wild type HIV-1 PR in these studies contains mutations Q7K, L33I, and L63I to diminish autoproteolysis and C67A and C95A to prevent cysteine-thiol oxidation, and showed almost identical kinetic parameters, stability and dimer dissociation as the unmutated wild type PR [31]. Kinetic parameters were measured for the resistant mutants and the wild type PR using the fluorescence substrate based on the p2-NC cleavage site of HIV-1 (Table 1). The mutants PR_{G48V}, PR_{I50V} and PR_{I54V} had reduced catalytic efficiency (k_{cat}/K_m) of about 10–40% of wild type PR value, while the catalytic efficiency of PR_{I54M} was similar to that of PR. The mutants showing reduced activity are likely to be less effective during viral replication.

The four mutants and the wild type PR were assayed for inhibition by saquinavir and darunavir (Table 1). Compared to wild type PR, mutant PR_{G48V} was poorly inhibited by saquinavir and darunavir with 90- and 30-fold higher inhibition constants (K_i), respectively. The K_i values of PR_{I50V} for saquinavir and darunavir were increased 30-fold and 24-fold, and the K_i values of PR_{I54V} were moderately increased by 8-fold and 15-fold for saquinavir and darunavir, relative to wild type PR values. In contrast, PR_{I54M} showed similar relative K_i values of 3 and 5for the two inhibitors. Therefore, the mutant PR_{G48V} was the most resistant to those inhibitors, while PR_{I54M} was the most similar to the wild type enzyme. PR_{I50V} was inhibited more effectively by saquinavir than by darunavir, in agreement with the presence of the I50V mutation in HIV isolates resistant to darunavir and its rarity in saquinavir treatment. However, PR_{G48V} was more susceptible to darunavir than saquinavir, in agreement with the presence of G48V in clinical isolates failing saquinavir therapy. Hence, darunavir is likely to be a better drug for patients carrying HIV PR with the G48V mutation selected by saquinavir treatment, while saquinavir may be better for resistant HIV with the I50V mutation.

Dimer Stability

The dimer stability of the four flap mutants (PR_{G48V}, PR_{I50V}, PR_{I54V}, and PR_{I54M}) and the wild type PR was evaluated by assessing the PR activity with increasing concentrations of denaturing urea. When the PR activity drops to 50% of the initial value, the concentration of urea is defined as UC_{50}. The UC_{50} value of PR_{I50V} was reduced to 60% of that for the wild type PR, while the UC_{50} values of the other three mutants were very similar to that of the wild type PR (90–110%). Earlier, we demonstrated that another flap mutant PR_{F53L} had reduced UC_{50} of 60% of the value for the wild type PR [13]. Therefore, the mutations of flap residues Ile50 and Phe53 adversely affect the PR dimer stability, while mutations G48V and I54V/M had no significant effect on the dimer stability in this assay.

Crystal Structures

The crystal structures of PR_{I50V}, PR_{I54V}, and PR_{I54M} complexed with saquinavir and PR_{G48V}, PR_{I54V}, and PR_{I54M} complexed with darunavir were determined at resolutions of 1.05–1.40 Å. No crystals were obtained for the complex of PR_{G48V} with saquinavir, and the structure of PR_{I50V} with darunavir was reported previously [11]. Three data sets (PR_{I54M}-SQV, PR_{I54V}-SQV, PR_{I54V}-DRV) reached atomic resolution (1.05 Å). The data collection and refinement statistics are provided in Table 2. All six structures crystallized in isomorphous unit cells and the same space group $P2_12_12$. The R-factors were refined to the range of 0.12 to 0.16. One asymmetric unit accommodated one PR dimer, with residues labeled 1–99 and 1′–99′ for each subunit. The electron density maps clearly showed the correct mutations in all the

complexes as illustrated in Figure 2. Most of the atoms were clearly visible in the electron density maps. An example from the flap region of PR_{I54V}-SQV is shown in Figure 2. Darunavir was bound at the active site of PR with two pseudosymmetric orientations in the complexes with PR_{G48V}, PR_{I54V}, and PR_{I54M}, while saquinavir showed a single orientation in the complexes of PR_{I54V}-SQV and two orientations in complexes of PR_{I54M}-SQV and PR_{I50V}-SQV. The omit maps of saquinavir (in PR_{I54V}-SQV) and darunavir (in PR_{I54V}-DRV) are shown in Figure 3. Alternate conformations were modeled for side chain and main chain atoms when observed in the electron density map. Met54 showed alternate conformations of the side chain only in the PR_{I54M}-SQV complex (Figure 2) and Val54 showed alternate conformations of the side chain only in PR_{I54V}-SQV complex. As frequently observed in near atomic resolution crystal structures, residue 50 showed alternate conformations for both main chain and side chain atoms in all complexes, except in the lower resolution structure of PR_{G48V}-DRV, 11; 13; 22. In addition, water molecules (161–223) and other solvent molecules including glycerol, phosphate, sodium ions and chloride ions with full or partial occupancy were modeled to fit the maps in the different structures.

Comparison of Protease Structures

The mutant PR complexes were compared to the PR structures with the corresponding inhibitor, which were determined in our previous studies. The same PR sequence is used to construct all mutants so any changes represent the effects of the introduced mutations. The wild type PR-DRV (2IEN) [21] structure has been solved at 1.30 Å resolution in space group $P2_12_12$, while the PR-SQV structure has been determined to 1.16 Å resolution in $P2_12_12_1$[22]. The mutations in the flap are expected to alter interactions with neighboring residues, the flap conformation and inhibitor binding. The overall structural differences between mutant PRs and the wild type PRs are shown by the RMS deviations, which do not reflect significant local differences, as observed in other PR structures [8; 12]. The pairwise overall RMS deviations of Cα were 0.1–0.3 Å for complexes with darunavir with the same unit cell and space group. The complex PR_{I54V}-DRV is the most similar to the wild type PR-DRV, while the other two complexes have similar deviations (0.3 Å) from the wild type PR. The pair-wise overall RMS deviations of Cα for the three complexes with saquinavir were very similar in the range of 0.6–0.7 Å, as observed for comparison of HIV PR structures in different space groups [13; 22; 32]. For all complexes, larger deviations were consistently located around the tip of the flap and 80's loop (residues 78–82) in both subunits. The alternate conformations of the main chain of residues 50/50′ contributed to the higher RMS deviations in the flaps. Structural differences for flap residues 47–54 are shown in Figure 4. PR_{G48V} had the biggest difference from the wild type PR among all the complexes with darunavir. The Cα atom of Ile50 shifted about 0.8 Å towards the active site cavity in one subunit and 0.5 Å at the equivalent position in the other subunit. In high resolution (better than 1.5 Å) structures, the atomic shifts over 0.3 Å are considered to be significant changes, using the estimation of crystallographic errors described in [33].

Notably, in all the mutant structures, the main chain atoms of residues 78–82 (the 80's loop) were shifted relative to their positions in wild type PR. The 80's loop shows intrinsic flexibility as described previously for atomic resolution structures of saquinavir complexes with wild type PR and mutants V82A and I84V [22] and a 9X mutant with indinavir [34]. The shifts appeared in both subunits of the dimer, and were slightly larger in one subunit than the other. The shifts of the 80's loop were related to the size of the side chain in the mutated residues, independent of the type of bound inhibitor. The 80's loop shifts away from a longer side chain (as in PR_{I54M}) and towards a smaller side chain (as in PR_{I54V}) to maintain the separation between residues 50, 54 and the 80's loop. However, the observed conformational changes in the 80's loop did not produce substantial changes in the interactions with inhibitors. Furthermore, the flap mutants showed varied effects for the interactions of the mutated residues with the bound inhibitors, as discussed for each mutant individually.

Protease Interactions with Saquinavir and Darunavir

The interatomic interactions that contribute to the binding of inhibitor in the active site cavity of PR include: strong N-H…O and O-H…O hydrogen bonds, weaker C-H…O, C-H…πinteractions, and the weakest van der Waals C-H…H-C contacts, as described previously for darunavir [12]. The different interactions are illustrated for the complexes of PR_{I54M} with the two inhibitors (Figure 5). Saquinavir with 49 non-hydrogen atoms is larger than darunavir with 38 non-hydrogen atoms. Saquinavir has larger hydrophobic groups at both ends of the molecule and forms more van der Waals interactions with numerous PR residues compared to darunavir [22]. Saquinavir forms eight direct hydrogen bonds, three water-mediated hydrogen bonds, and one C-H…O interaction with Gly 49. However, darunavir forms two more direct hydrogen bonds with the main chain atoms of Asp29 and Asp30 and two more C-H…O interactions with main chain atoms than does saquinavir [21; 22]. Similar hydrogen bond interactions are retained in the inhibitor complexes with wild type protease and the other mutants. The only exception is the interaction of the aniline NH2 of darunavir with the carboxylate oxygen of Asp30, which is a direct hydrogen bond in the wild type and other mutant complexes, and a water-mediated interaction for the major darunavir conformation in the PR_{I54M}-DRV complex. The van der Waals and C-H…π interactions between PR and hydrophobic groups of saquinavir are likely to be vulnerable to changes due to mutations of hydrophobic residues in the binding site. On the contrary, darunavir was designed to form more hydrogen bond interactions with main-chain atoms of PR, which cannot be directly altered by mutations [23]. Therefore, the binding of darunavir can adapt to the changes due to mutations of hydrophobic residues in the active site cavity. Through this strategy darunavir retains its effectiveness for many drug resistant mutants, with the exception of PR_{I50V} due to the loss of hydrogen bond interactions 11; 20; 21. However, altered interactions are observed in some mutant complexes as described in the following sections, which are organized by individual mutants.

PR_{G48V}-DRV—Residue Gly48 is located in the active site cavity and its carbonyl O makes C-H…O interactions with darunavir in the wild type PR complexes. Replacing Gly48 by Val in PR_{G48V} is expected to disrupt the interactions with neighboring residues on the flap, and possibly alter the interactions with the inhibitor, thus destabilizing the flap and reducing the affinity for inhibitor. Despite extensive efforts, no crystals were obtained for the single mutant PR_{G48V} in complex with saquinavir. Fortunately, crystals were obtained for PR_{G48V} with darunavir that diffracted to 1.40 Å. The comparison of PR_{G48V}-DRV with the wild type PR-DRV complex showed that the Cα of Val48 in both subunits had lost interactions with the Phe53 aromatic ring, while new hydrophobic interactions were observed for the Val48 side chain (Figure 6a). In one subunit, residues Gly49 and Ile50 have shifted 0.7 Å away from the neighboring residues Gly52 and Phe53, while there is relatively little change in the position of the Phe53 side chain relative to the wild type. As a result, the Cα of Val48 has lost most of the favorable C-H…π interactions with the aromatic ring of Phe53. However, the Cβ and Cγ atoms of Val48 have gained new interactions with the aromatic ring of Phe53. In the other subunit, the side chain of Phe53′ had rotated about 180° relative to its position in the wild type PR, which eliminated C-H…πinteractions with the Cα of Gly48′. However, a new C-H…O interaction was formed between the Cγ of Val48′ and the carbonyl O of Gly52′, which partially compensated for the lost contacts. Thus, the introduction of the larger Val side chain at position 48 has disturbed the interactions with the neighboring residues in the complex of PR_{G48V}-DRV, while structural adjustments partially compensated for lost interactions.

Other structural changes in the PR_{G48V}-DRV complex were observed for the 80's loop. Residue 48 is located near the 80's loop of the same PR subunit, but no van der Waals contacts shorter than 4.2 Å were observed between the two regions. In the mutant, the 80's loop has shifted up to 0.7 Å towards Val48 relative to its position in the wild type structure; nevertheless the residues remained too far apart to make favorable interactions.

The main chain carbonyl group of Gly48 makes direct interactions with the major (60%) and minor (40%) orientations of darunavir, as shown in Figure 5b. In the mutant the main chain atoms of Val48 have shifted by as much as 0.9 Å at the carbonyl oxygen relative to their positions in wild type PR-DRV structure. As a result, the carbonyl oxygen of Val48 has gained additional interactions with darunavir, which are not observed in the wild type structure. There are several shorter and stronger C-H…O interactions with the minor orientation of darunavir, and the side chain of Val48 has gained a new van der Waals interaction with the aromatic ring of the inhibitor (Figure 6b). On the other hand, the major orientation has similar contacts to those of the wild-type complex. However, the favorable interactions described above are likely offset by several repulsive short C-H…H-C hydrophobic contacts made with the side chain atoms of Pro81, Pro81′ and Ile84′. The P1 benzene ring of darunavir in both orientations is involved in short 3.1–3.5 Å contacts with residues 81 and 81′, while the aniline part of the minor darunavir orientation makes very short (2.7–3.2 Å) interactions with Cδ of Ile84′. These short contacts were not observed in the wild type PR-DRV structures or other mutant complexes examined [11; 12; 13; 35]. Therefore, PR_{G48V}-DRV represents a unique structure with unfavorably close PR-ligand interactions, rather than longer or lost contacts as observed in other mutant complexes. In agreement with the structural changes, the K_i value for the PR_{G48V} inhibition by darunavir increased ~ 30 times relative to the wild type PR, suggesting that the repulsive contacts have a significantly negative effect on the darunavir affinity for the mutant PR.

The crystal structure of PR_{G48V}-SQV is not available for comparison. However, the crystal structure of the double mutant $PR_{G48V/L90M}$ with SQV (1FB7) shows that saquinavir moves to accommodate the bigger side chain of Val48, giving rise to weaker interactions than in the PR-SQV structure [30]. The carbonyl O of Val48 loses the hydrogen bond interaction with SQV. In addition, there are fewer van der Waals interactions between saquinavir and the flap (residues 47–50). These structural changes and reduced protease-inhibitor interactions, including loss of a hydrogen bond, explain why G48V is a primary mutation observed in isolates that are resistant to saquinavir. On the other hand, the G48V mutation is not considered to be resistant to darunavir, although potentially repulsive protease-inhibitor contacts were observed in the new structure of PR_{G48V}-DRV.

PR_{I50V} Complexes—The new structure of PR_{I50V}-SQV is described and compared with the structure of PR_{I50V}- DRV (2FGG). Residue 50 lies at the tip of the flap and the carbonyl oxygen forms a hydrogen bond interaction with the main chain amide of Gly51′ from the other subunit. The role of Ile/Val50 in binding of indinavir or darunavir has been described previously [11; 13]. In the wild type PR, the side chain of Ile50 forms van der Waals interactions with Thr80′ and Pro81′. Thr80 has been proposed to maintain the mobility of the flap tips by pulling Ile50′ of the other subunit out of a hydrophobic pocket [36]. In PR_{I50V}-SQV, the smaller side chain in Val50 has induced a shift towards the 80's loop to maintain favorable contacts (Figure 7a). Moreover, the side chain of Val50 has rotated to gain van der Waals interactions with Ile54′. Therefore, the PR_{I50V}-SQV structure shows adaptations to improve intersubunit contacts, unlike the PR_{I50V}-indinavir complex that showed reduced contacts between the two subunits at the flap tip [13].

Overall, the interactions of PR_{I50V} and saquinavir show little change relative to those of wild type PR-SQV, even for residue 50. Val50 in one subunit has lost two van der Waals interactions with saquinavir compared with those of Ile50, while in the other subunit this residue has gained a new van der Waals interaction with saquinavir. In contrast, our previous studies showed that several attractive interactions between the side chain of Ile50 and inhibitor were lost in the complexes of PR_{I50V} with darunavir and indinavir 11; 13. Moreover, the aniline of darunavir had lost two hydrogen bonds with the main chain of Asp30, in agreement with the higher relative Ki for the mutant. All three inhibitors show reduced interactions and higher relative

Ki values forPR_{I50V} compared to wild type enzyme. However, the loss of hydrogen bonds in the mutant PR_{I50V}-DRV complex is consistent with the presence of this mutation in isolates resistant to darunavir. Also, the absence of large structural changes in the saquinavir complex agrees with the rarity of the I50V mutation during resistance to saquinavir.

PR_{I54M} and PR_{I54V} complexes with DRV and SQV—Residue 54 is located on the opposite side of the flap from residue 48, and close to residue 50 and the 80's loop (Figure 1). Significant structural changes were observed at the 80's loop in the complexes of mutants with saquinavir and darunavir in comparison with the corresponding wild type PR complexes (Figure 7). The 80's loop was shifted away from Met54 in PR_{I54M} and towards Val54 in PR_{I54V} to compensate for the different sizes of the side chains of residue 54. In PR_{I54M}-DRV, the carbonyl O of Pro79 has shifted away from the longer Met54 by 0.7 Å and 1.4 Å in the two subunits, respectively, in order to accommodate the longer Met side chain. Despite this movement, Met54 has gained more van der Waals contacts with Pro79 and the side chain of Ile50′ than are observed for wild type Ile54. Moreover, the flap tip has shifted towards Met54 by 0.5 Å at the carbonyl O of Gly51, because there is more space due to the absence of the β-branched methyl group of Ile in Met54. On the other hand, the mutation I54V introduces a smaller side chain, so the 80's loop has shifted towards Val54 by 0.6 Å at the carbonyl O of Pro79′ in only one subunit of PR_{I54V}-DRV. However, no new interactions are formed between Val54 and the 80's loop (Figure 7c). Unlike in PR_{I54M}-DRV, the tip of the flap had no significant change in PR_{I54V}–DRV relative to the wild type PR structure.

The shift of the 80's loop caused by the mutation of residue 54 has modified the interactions with inhibitor in PR_{I54M}DRV, but not in the other complexes. In PR_{I54M}-DRV, residues 78–82 were further away from 54 in the flap, so the interactions between Pro81-Val82 and the major conformation of darunavir were a little weaker (the interatomic distances are 0.3–0.4 Å longer) than in the wild type complex. For the major conformation of darunavir, the direct hydrogen bond interaction between the aniline NH2 of darunavir and OD2 of Asp30 in the wild type PR was replaced by a water-mediated interaction in PR_{I54M}-DRV (Figure 5). For the minor conformation of darunavir, however, the direct hydrogen bond interaction was maintained, while the hydrogen bond interaction between the NH2 of darunavir and the carbonyl O of Asp30 was lost (interatomic distance is 4.5 Å). On the other hand, no significant structural changes in the PR-inhibitor interactions were observed in the PR_{I54V}-DRV, PR_{I54V}-SQV and PR_{I54M}-SQV complexes relative to the corresponding wild type PR complexes. In summary, the I54M mutation caused larger structural changes than I54V in the flap and in the interactions with darunavir, which is consistent with the more frequent occurrence of mutation I54M compared to I54V in the treatment with amprenavir and darunavir [28].

Structural and kinetic changes and drug resistance

These new crystal structures of the drug resistant mutants revealed changes in PR conformation and interaction with inhibitor relative to the equivalent wild type PR complexes. The introduction of mutations in the flap caused conformational modifications of the flap in all the complexes, with the biggest deviations observed in the PR_{G48V}-DRV complex. In all the complexes, the 80's loop has flexibly adjusted to accommodate the size of neighboring residues 50 and 54. It shifted towards smaller residues like Val50 and Val54, and away from the longer residue Met54. However, the shifts of the 80's loop did not significantly alter the interactions between inhibitor and PR, except in the cases of PR_{G48V}-DRV and PR_{I54M}-DRV. The van der Waals interactions with darunavir were enhanced in PR_{G48V}-DRV but were weakened slightly in PR_{I54M}-DRV in correlation with the shift of the 80's loop.

Analysis of the available structures of these flap mutants with saquinavir or darunavir showed the largest changes in $PR_{G48V/L90M}$-SQV [30] and PR_{I50V}–DRV relative to the corresponding wild type complexes [11]. In both cases, at least one PR-inhibitor hydrogen bond interaction is eliminated in the mutant complex, and the differences relate to the chemical structures of the two drugs. One notable difference is that saquinavir forms one hydrogen bond with the carbonyl O of Gly48, while this interaction is replaced by two weaker CH…O interactions in the darunavir complexes. The hydrogen bond between Gly48 and saquinavir was absent in the structure of $PR_{G48V/L90M}$-SQV [30], consistent with the 90-fold reduced inhibition. However, the CH…O interactions between Val48 and darunavir in PR_{G48V}-DRV were even tighter than in the wild type PR-DRV. This difference in polar interactions may explain why PR_{G48V} provides resistance to saquinavir yet maintains susceptibility to darunavir. The opposite occurs with the mutant PR_{I50V}; the darunavir complex has lost hydrogen bond, as well as van der Waals interactions, while only a few changes in hydrophobic interactions were seen in the saquinavir complex. The loss of hydrogen bond interactions with inhibitor in PR_{I50V} appears to provide resistance to darunavir, and in $PR_{G48V/L90M}$ to provide resistance to saquinavir, as suggested in previous studies [11; 30].

Saquinavir appeared to adapt better than darunavir to the changes caused by I54M and I54V, which is consistent with the increased prevalence of both mutations in HIV isolates showing resistance to darunavir. PR_{I54M} showed reduced van der Waals interactions with darunavir in correlation with the shift of the 80's loop, and both darunavir conformations had lost a direct hydrogen bond with Asp30. However, no significant reduction in inhibitor interactions was observed in the structures of PR_{I54V}-DRV, PR_{I54V}-SQV and PR_{I54M}-SQV.

The observed changes in PR structure and activity in the flap mutants PR_{G48V}, PR_{I50V}, PR_{I54V}, and PR_{I54M} are in good agreement with the occurrence of these mutations in drug resistance to darunavir and saquinavir. In addition to these structural changes, several other factors must be considered since drug resistance to PR inhibitors can arise by various molecular mechanisms, including reduced inhibition, altered PR activity and stability [8; 13; 14]. The structure and activity of PR is especially sensitive to mutations in the flap region, consistent with their frequent appearance in drug resistant HIV [6]. In fact, PR_{G48V}, PR_{I50V} and PR_{I54V} showed reduced catalytic efficiency and PR_{I50V} had reduced stability, and these mutations are likely to be deleterious for correct polyprotein processing and viral replication. Such unfavorable mutations will only be selected under the severe pressure of drug treatment. The Ile54 mutants showed relatively small changes in inhibition by saquinavir and darunavir, and the mutants are similar to wild type in catalytic activity and stability. However, PR_{I54M} showed significant structural changes and reduced polar interactions with darunavir consistent with clinical resistance data. Moreover, an unusual mechanism for resistance was proposed for mutant PR_{I54V}, which showed fewer hydrogen bonds with a peptide reaction intermediate [37]. The interactions with substrates or reaction intermediates have not been investigated for other mutants.

These new structures revealed that saquinavir and darunavir differ in their interactions with specific mutants. Importantly, saquinavir showed reduced inhibition and hydrogen bond interactions for mutants containing G48V and less change with PR_{I50V}, while the opposite is seen for darunavir, in excellent agreement with the resistance data and despite the reduced activity of these mutants. Overall, the changes in polar interactions between PR mutants and inhibitor have the best correlation with observed resistance mutations. Therefore, this structural analysis will assist with predictive genotyping of clinical isolates and in the development of new protease inhibitors to combat HIV drug resistance.

MATERIALS AND METHODS

Preparation of HIV-1 Protease Mutants

The optimized HIV-1 PR clone with mutations Q7K, L33I, and L63I to diminish the autoproteolysis of the PR, as well as mutations C67A and C95A to prevent cysteine-thiol oxidation was used as the initial template for adding drug resistant mutations [31]. This optimized PR had almost identical kinetic parameters and stability with the mature PR (Genbank HIVHXB2CG) [31]. Plasmid DNA (pET11a, Novagen) encoding PR was utilized to construct mutant PR by the Quick-Change mutagenesis kit (Stratagene). The PR mutants were expressed in *Escherichia coli* BL21 (DE3) and the protein was purified from inclusion bodies as described [38]. The presence of the appropriate mutations was confirmed by DNA sequencing.

Enzyme Kinetic Assays

Kinetic parameters were determined by a fluorescence assay. The substrate was Abz-Thr-Ile-Nle-pNO2Phe-Gln-Arg-NH2, where Abz is anthranylic acid, Nle is norleucine, based on the p2-NC cleavage site of the natural polyprotein substrate. Protease (10 μl, final concentration of ~20–70 nM) was mixed with 98 μl reaction buffer (100 mM MES, pH=5.6, 400 mM NaCl, 1 mM EDTA, 5% glycerol) and 2 μl of DMSO or inhibitor in DMSO, and the mixture was preincubated at 26°C for 5 min. The reaction was initiated by adding 90 μl of substrate from stock solution of 240 μM (final concentration of 10–70 μM), due to the solubility limit of substrate. The resulting mixture was assayed over 5 min for the increase in fluorescence using 340 nM and 420 nM bandpass filters for the excitation and emission. Data analysis was performed with the program SigmaPlot 8.02. k_{cat} and K_m values were obtained by standard data-fitting techniques for a reaction obeying Michaelis-Menten kinetics. K_i values were obtained from the IC_{50} values estimated from an inhibitor dose-response curve with the fluorescent assay using the equation $K_i = (IC_{50} - [E]/2)/(1 + [S]/K_m)$, where [E] and [S] are the protease and substrate concentrations, respectively [39].

Urea Denaturation Assay

The effect of urea denaturation was measured using the spectroscopic assay [14]. The decrease of absorbance of chromogenic substrate (The Lys-Ala-Arg-Val-Nle-p-nitroPhe-Glu-Ala-Nle-amide, where Nle is norleucine) was monitored at 310 nm by a PerkinElmer Lambda 35 UV/Vis spectrophotometer. The substrate was concentrated at 400 μM and PR activity was measured at urea concentration of 0–3.0 M with a final enzyme concentration of 300–500 nM. The UC_{50} values were determined by plotting the initial velocities against increasing urea concentration using SigmaPlot 8.02.

Crystallographic Analysis

PR_{I50V}, PR_{I54V} and PR_{I54M} were cocrystallized with saquinavir, while PR_{G48V}, PR_{I54V} and PR_{I54M} were cocrystallized with darunavir at room temperature by the hanging drop method. The protein (2–5 mg/ml) was preincubated with the inhibitor in a molar ratio of 1:5–10. The crystallization drops had a 1:1 ratio by volume of reservoir solution and protein. For PR_{I50V} - SQV, the reservoir contained 0.2 M sodium citrate, phosphate buffer, pH 6.0–6.2 and 30–35% saturated ammonium sulfate as precipitant; For PR_{I54V}-SQV, 0.1 M sodium acetate buffer, pH 5.4, 1M NaCl as precipitant; For PR_{I54M}-SQV, 0.2 M sodium acetate buffer, pH 4.8–5.2 and 10–15% NaCl as precipitant; For PR_{I50V}-DRV, 0.2M sodium citrate, phosphate buffer, pH 6.0–6.2 and 30–35% saturated $(NH_4)_2SO4$ as precipitant; For PR_{G48V}-DRV, 0.1 M citrate/0.2 M phosphate buffer, pH 5.6–5.8, 1.3M KCl as precipitant and 7–10% MPD; For PR_{I54V}-DRV, 0.1 M sodium acetate buffer, pH 4.4, 1M NaCl as precipitant; For PR_{I54M}-DRV, 0.2 M sodium acetate buffer, pH 4.4–4.6, 25–30% NaCl as precipitant. The crystals grew from overnight to 10 days into bricks, plates, and rod shapes. Some of them formed crystal clusters and were cut

into individual crystals before mounting. Crystals were frozen in liquid nitrogen after soaking in 20–35% glycerol as a cryoprotectant.

X-ray diffraction data for all the complexes were collected on the SER-CAT ID beamline of the Advanced Photon Source, Argonne National Laboratory. Data were processed using HKL2000[40], and the structures were solved by molecular replacement using CCP4i [41; 42], refined using SHELX [43] and refitted using O [44]. Alternate conformations for residues were modeled according to the electron density maps. Anisotropic B factors were refined for all the structures. Hydrogen atom positions were included in the last stage of refinement using all data.

The mutant crystal structures were compared with the wild type by superimposing their Cα atoms on each other and structural figures were made using Bobscript [45; 46] and PyMOL [47].

Protein Data Bank Accession Codes

The atomic coordinates and structure factors have been deposited in the Protein Data Bank with accession code 3CYX for PR_{I50V}-SQV, 3D1Y for PR_{I54V}-SQV, 3D1X for PR_{I54M}-SQV, 3CYW for PR_{G48V}-DRV, 3D20 for PR_{I54V}-DRV and 3D1Z for PR_{I54M}-DRV, respectively.

Acknowledgments

We thank the staff at the SER-CAT beamline at the Advanced Photon Source, Argonne National Laboratory, for assistance during X-ray data collection. Use of the Advanced Photon Source was supported by the U. S. Department of Energy, Office of Science, Office of Basic Energy Sciences, under Contract No. DE-AC02–06CH11357. The research was supported in part by the Georgia State University Molecular Basis of Disease Program, the Georgia Research Alliance, the Georgia Cancer Coalition, and the National Institute of Health grants GM062920 and GM053386.

Abbreviations

HIV-1
: human immunodeficiency virus type 1

PR
: HIV-1 protease

PR_{G48V}
: PR with G48V mutation

PR_{I50V}
: PR with I50V mutation

PR_{I54V}
: PR with I54V mutation

PR_{I54M}
: PR with I54M mutation

RMS
: root mean square

References

1. Miller M, Schneider J, Sathyanarayana BK, Toth MV, Marshall GR, Clawson L, Selk L, Kent SB, Wlodawer A. Structure of complex of synthetic HIV-1 protease with a substrate-based inhibitor at 2.3 A resolution. Science 1989;246:1149–52. [PubMed: 2686029]

2. Gustchina A, Weber IT. Comparison of inhibitor binding in HIV-1 protease and in non-viral aspartic proteases: the role of the flap. FEBS 1990;269:269–272.

3. Ishima R, Freedberg DI, Wang YX, Louis JM, Torchia DA. Flap opening and dimer-interface flexibility in the free and inhibitor-bound HIV protease. Structure 1999;7:1047–55. [PubMed: 10508781]

4. Shao W, Everitt L, Manchester M, Loeb DD, Hutchison CA 3rd, Swanstrom R. Sequence requirements of the HIV-1 protease flap region determined by saturation mutagenesis and kinetic analysis of flap mutants. Proc Natl Acad Sci 1997;94:2243–8. [PubMed: 9122179]

5. Shafer RW. Genotypic testing for human immunodeficiency virus type 1 drug resistance. Clin Microbiol Rev 2002;15:247–77. [PubMed: 11932232]

6. Shafer RW, Rhee SY, Pillay D, Miller V, Sandstrom P, Schapiro JM, Kuritzkes DR, Bennett D. HIV-1 protease and reverse transcriptase mutations for drug resistance surveillance. Aids 2007;21:215–23. [PubMed: 17197813]

7. Heaslet H, Rosenfeld R, Giffin M, Lin YC, Tam K, Torbett BE, Elder JH, McRee DE, Stout CD. Conformational flexibility in the flap domains of ligand-free HIV protease. Acta Crystallogr D Biol Crystallogr 2007;63:866–75. [PubMed: 17642513]

8. Liu F, Kovalevsky AY, Louis JM, Boross PI, Wang YF, Harrison RW, Weber IT. Mechanism of Drug Resistance Revealed by the Crystal Structure of the Unliganded HIV-1 Protease with F53L Mutation. J Mol Biol 2006;358:1191–9. [PubMed: 16569415]

9. Logsdon BC, Vickrey JF, Martin P, Proteasa G, Koepke JI, Terlecky SR, Wawrzak Z, Winters MA, Merigan TC, Kovari LC. Crystal structures of a multidrug-resistant human immunodeficiency virus type 1 protease reveal an expanded active-site cavity. J Virol 2004;78:3123–32. [PubMed: 14990731]

10. Prabu-Jeyabalan M, Nalivaika EA, Romano K, Schiffer CA. Mechanism of substrate recognition by drug-resistant human immunodeficiency virus type 1 protease variants revealed by a novel structural intermediate. J Virol 2006;80:3607–16. [PubMed: 16537628]

11. Kovalevsky AY, Tie Y, Liu F, Boross PI, Wang YF, Leshchenko S, Ghosh AK, Harrison RW, Weber IT. Effectiveness of nonpeptide clinical inhibitor TMC-114 on HIV-1 protease with highly drug resistant mutations D30N, I50V, and L90M. J Med Chem 2006;49:1379–87. [PubMed: 16480273]

12. Kovalevsky AY, Liu F, Leshchenko S, Ghosh AK, Louis JM, Harrison RW, Weber IT. Ultra-high Resolution Crystal Structure of HIV-1Protease Mutant Reveals Two Binding Sites for Clinical Inhibitor TMC114. J Mol Biol 2006;363:161–173. [PubMed: 16962136]

13. Liu F, Boross PI, Wang YF, Tozser J, Louis JM, Harrison RW, Weber IT. Kinetic, stability, and structural changes in high-resolution crystal structures of HIV-1 protease with drug-resistant mutations L24I, I50V, and G73S. J Mol Biol 2005;354:789–800. [PubMed: 16277992]

14. Mahalingam B, Louis JM, Reed CC, Adomat JM, Krouse J, Wang YF, Harrison RW, Weber IT. Structural and kinetic analysis of drug resistant mutants of HIV-1 protease. Eur J Biochem 1999;263:238–245. [PubMed: 10429209]

15. Wang YF, Tie Y, Boross PI, Tozser J, Ghosh AK, Harrison RW, Weber IT. Potent new antiviral compound shows similar inhibition and structural interactions with drug resistant mutants and wild type HIV-1 protease. J Med Chem 2007;50:4509–15. [PubMed: 17696515]

16. Buonaguro L, Tornesello ML, Buonaguro FM. Human immunodeficiency virus type 1 subtype distribution in the worldwide epidemic: pathogenetic and therapeutic implications. J Virol 2007;81:10209–19. [PubMed: 17634242]

17. Coman RM, Robbins AH, Fernandez MA, Gilliland CT, Sochet AA, Goodenow MM, McKenna R, Dunn BM. The contribution of naturally occurring polymorphisms in altering the biochemical and structural characteristics of HIV-1 subtype C protease. Biochemistry 2008;47:731–43. [PubMed: 18092815]

18. Sanches M, Krauchenco S, Martins NH, Gustchina A, Wlodawer A, Polikarpov I. Structural characterization of B and non-B subtypes of HIV-protease: insights into the natural susceptibility to drug resistance development. J Mol Biol 2007;369:1029–40. [PubMed: 17467738]

19. De Meyer S, Azijn H, Surleraux D, Jochmans D, Tahri A, Pauwels R, Wigerinck P, de Bethune MP. TMC114, a novel human immunodeficiency virus type 1 protease inhibitor active against protease inhibitor-resistant viruses, including a broad range of clinical isolates. Antimicrob Agents Chemother 2005;49:2314–21. [PubMed: 15917527]

20. Koh Y, Nakata H, Maeda K, Ogata H, Bilcer G, Devasamudram T, Kincaid JF, Boross P, Wang YF, Tie Y, Volarath P, Gaddis L, Harrison RW, Weber IT, Ghosh AK, Mitsuya H. A novel bis-tetrahydrofuranylurethane-containing nonpeptidic protease inhibitors (PI) UIC-94017 (TMC114) potent against multi-PI-resistant HIV in vitro. Antimicrob Agents Chemother 2003;47:3123–3129. [PubMed: 14506019]
21. Tie Y, Boross PI, Wang YF, Gaddis L, Hussain AK, Leshchenko S, Ghosh AK, Louis JM, Harrison RW, Weber IT. High resolution crystal structures of HIV-1 protease with a potent non-peptide inhibitor (UIC-94017) active against multi-drug-resistant clinical strains. J Mol Biol 2004;338:341–52. [PubMed: 15066436]
22. Tie Y, Kovalevsky AY, Boross PI, Wang YF, Ghosh AK, Tozser J, Harrison RW, Weber IT. High Resolution Crystal Structures of HIV-1 Protease and Mutants V82A and I84V with Saquinavir. Proteins: Structure, Function, and Bioinformatics. 2006in press
23. Ghosh AK, Dawson ZL, Mitsuya H. Darunavir, a conceptually new HIV-1 protease inhibitor for the treatment of drug-resistant HIV. Bioorg Med Chem 2007;15:7576–80. [PubMed: 17900913]
24. Noble S, Foulds D. Saquinavir: a review of its pharmacology and clinical potential in the management of HIV infection. Drugs 1996;52:93–112. [PubMed: 8799687]
25. Shapiro JM, Winters MA, Lawrence J, Merigan TC. Clinical cross-resistance between the HIV-1 protease inhibitors saquinavir and indinavir and correlations with genotypic mutations. AIDS 1999;13:359–65. [PubMed: 10199226]
26. Condra JH, Petropoulos CJ, Ziermann R, Schleif WA, Shivaprakash M, Emini EA. Drug resistance and predicted virologic responses to human immunodeficiency virus type 1 protease inhibitor therapy. J Infect Dis 2000;182:758–765. [PubMed: 10950769]
27. Molla A, Korneyeva M, Gao Q, Vasavanonda S, Schipper PJ, Mo HM, Markowitz M, Chernyavskiy T, Niu P, Lyons N, Hsu A, Granneman GR, Ho DD, Boucher CA, Leonard JM, Norbeck DW, Kempf DJ. Ordered accumulation of mutations in HIV protease confers resistance to ritonavir. Nat Med 1996;2:760–6. [PubMed: 8673921]
28. Murphy MD, Marousek GI, Chou S. HIV protease mutations associated with amprenavir resistance during salvage therapy: importance of I54M. J Clin Virol 2004;30:62–7. [PubMed: 15072756]
29. Lambert-Niclot S, Flandre P, Canestri A, Peytavin G, Blanc C, Agher R, Soulie C, Wirden M, Katlama C, Calvez V, Marcelin AG. Factors Associated with the Selection of Mutations Conferring Resistance to Protease Inhibitors (PIs) in PI-Experienced Patients Displaying Treatment Failure on Darunavir. Antimicrob Agents Chemother 2008;52:491–6. [PubMed: 18039922]
30. Hong L, Zhang XC, Hartsuck JA, Tang J. Crystal structure of an in vivo HIV-1 protease mutant in complex with saquinavir: insights into the mechanisms of drug resistance. Protein Sci 2000;9:1898–904. [PubMed: 11106162]
31. Louis JM, Clore GM, Gronenborn AM. Autoprocessing of HIV-1 protease is tightly coupled to protein folding. Nat Struct Biol 1999;6:868–875. [PubMed: 10467100]
32. Zoete V, Michielin O, Karplus M. Relation between sequence and structure of HIV-1 protease inhibitor complexes: a model system for the analysis of protein flexibility. J Mol Biol 2002;315:21–52. [PubMed: 11771964]
33. Weber, IT.; Kovalevsky, AY.; Harrison, RW. Structures Of HIV Protease Guide Inhibitor Design To Overcome Drug Resistance. In: Caldwell, GW.; Atta-ur-Rahman; Player, MR.; Choudhary, MI., editors. Frontiers in Drug Design and Discovery. Vol. 3. Bentham Science Publishers; 2007. p. 45-62.
34. Munshi S, Chen Z, Yan Y, Li Y, Olsen DB, Schock HB, Galvin BB, Dorsey B, Kuo LC. An alternate binding site for the P1-P3 group of a class of potent HIV-1 protease inhibitors as a result of concerted structural change in the 80s loop of the protease. Acta Crystallogr D Biol Crystallogr 2000;56:381–8. [PubMed: 10739910]
35. Tie Y, Boross PI, Wang YF, Gaddis L, Liu F, Chen X, Tozser J, Harrison RW, Weber IT. Molecular basis for substrate recognition and drug resistance from 1.1 to 1.6 angstroms resolution crystal structures of HIV-1 protease mutants with substrate analogs. FEBS J 2005;272:5265–77. [PubMed: 16218957]
36. Foulkes JE, Prabu-Jeyabalan M, Cooper D, Henderson GJ, Harris J, Swanstrom R, Schiffer CA. Role of invariant Thr80 in human immunodeficiency virus type 1 protease structure, function, and viral infectivity. J Virol 2006;80:6906–16. [PubMed: 16809296]

37. Kovalevsky AY, Chumanevich AA, Liu F, Louis JM, Weber IT. Caught in the Act: the 1.5 A resolution crystal structures of the HIV-1 protease and the I54V mutant reveal a tetrahedral reaction intermediate. Biochemistry 2007;46:14854–64. [PubMed: 18052235]

38. Mahalingam B, Louis JM, Hung J, Harrison RW, Weber IT. Structural implications of drug resistant mutants of HIV-1 protease: High resolution crystal structures of the mutant protease/substrate analog complexes. Proteins: Structure, Function, and Genetics 2001;43:455–464.

39. Maibaum J, Rich DH. Inhibition of porcine pepsin by two substrate analogues containing statine: the effect of histidine at the P2 subsite on the inhibition of aspartic proteinases. J Med Chem 1988;31:625–629. [PubMed: 3126296]

40. Otwinowski Z, Minor W. Processing of X-ray diffraction data in oscillation mode. Methods in Enzymology 1997;276:307–326.

41. Collaborative Computational Project N. The CCP4 Suite: Programs for Protein Crystallography. Acta Cryst D 1994;50:760–3. [PubMed: 15299374]

42. Potterton E, Briggs P, Turkenburg M, Dodson EA. Graphical user interface to the CCP4 program suite. Acta Cryst D 2003;59:1131–7. [PubMed: 12832755]

43. Sheldrick GM, Schneider TR. High resolution refinement. Methods in Enzymology 1997;277:319–343. [PubMed: 18488315]

44. Jones TA, Zou JY, Cowan SW, Kjeldgaard M. Improved methods for building protein models in electron density maps and the location of errors in these models. Acta Crystallog 1991;A47:110–119.

45. Esnouf RM. An extensively modified version of MolScript that includes greatly enhanced coloring capabilities. J Mol Graph Model 1997;15:132–4. [PubMed: 9385560]

46. Esnouf RM. Further additions to MolScript version 1.4, including reading and contouring of electron-density maps. Acta Cryst 1999;D55:938–940.

47. DeLano, WL. The PyMOL Molecular Graphics System. 2002. http://www.pymol.org

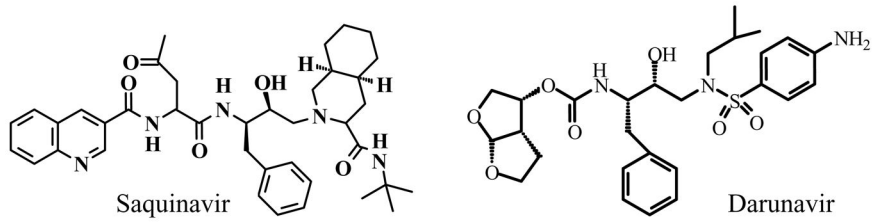

(a)

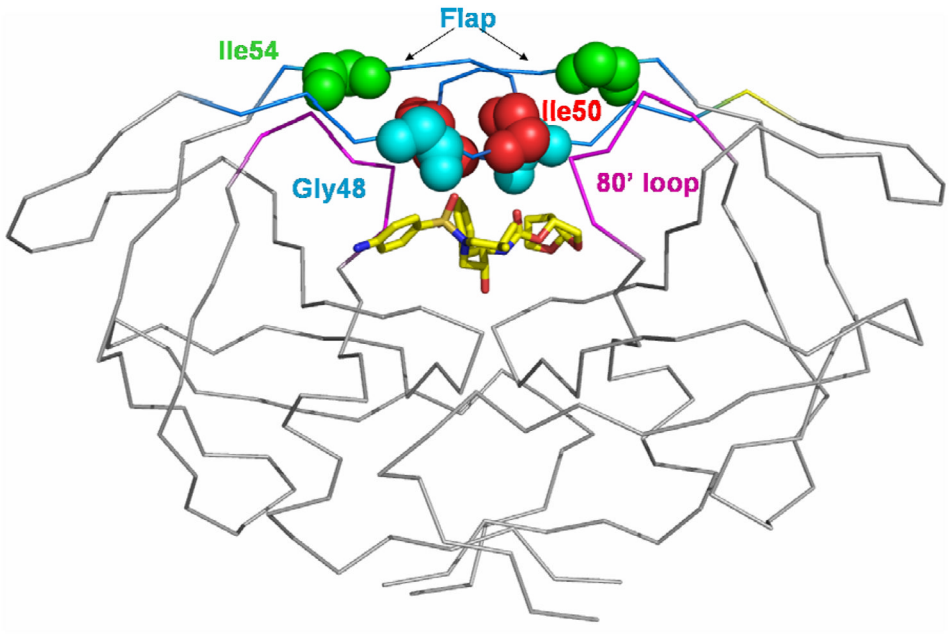

(b)

Figure 1.

(a) The chemical structures of saquinavir and darunavir. (b) Structure of HIV-1 PR dimer with the locations of mutated residues Gly48 (cyan), Ile50 (red), Ile54 (green) indicated by spheres for main chain atoms in both subunits. Darunavir is shown in sticks colored by atom type. The flap residues (45–55) and the 80's loop (78–82) are colored in blue and purple, respectively.

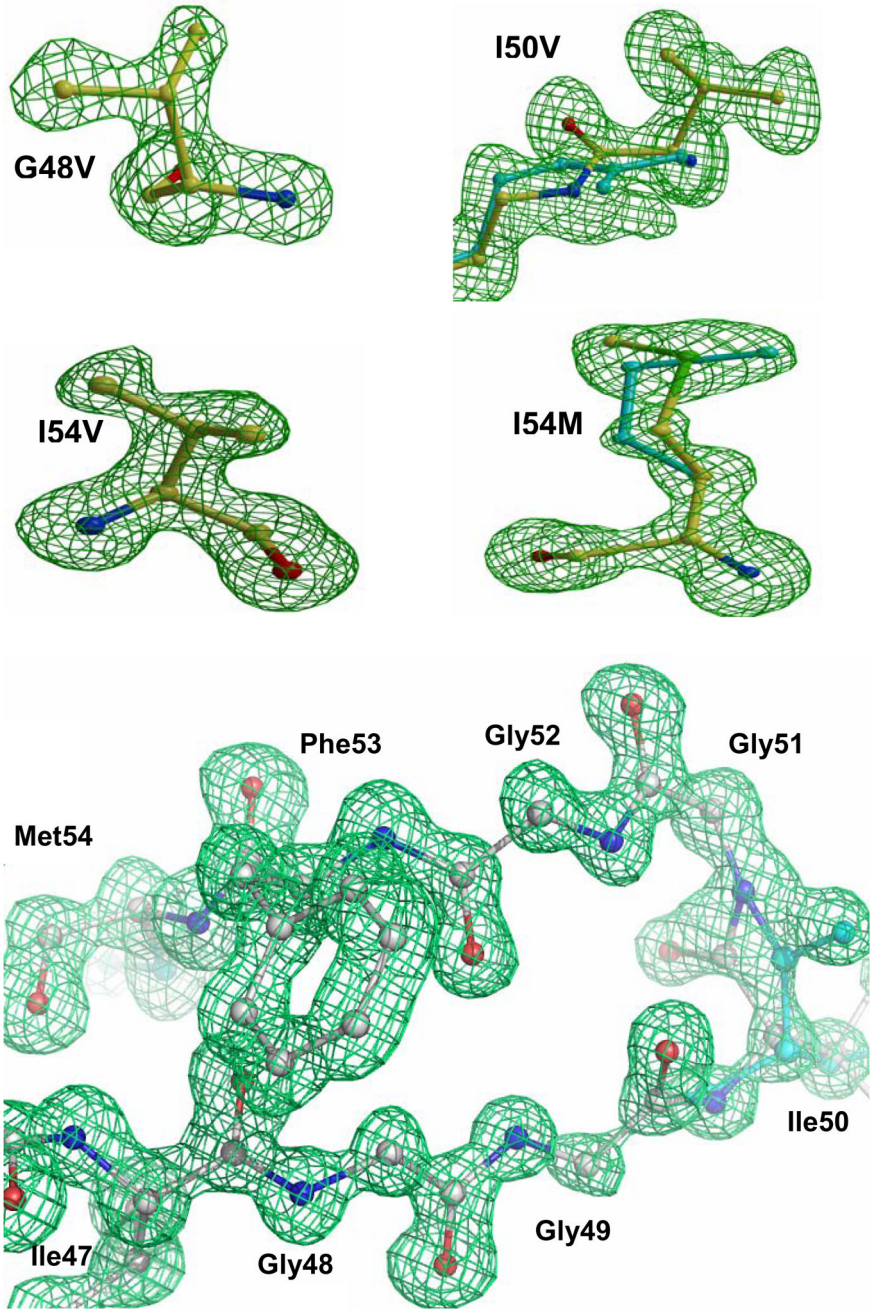

Figure 2.

The Fo-Fc omit maps showing the mutated residues and the flap residues (47–54) contoured at 3.3 sigma. Val 48 is from PR_{G48V}-DRV, Val50 from PR_{I50V}-SQV, Val54 from PR_{I54V}-SQV, Met54 from PR_{I54M}-SQV and flap residues from PR_{I54M}-SQV. The cyan sticks indicate the alternate conformations of main-chain and side-chain atoms in Val50 and Met54.

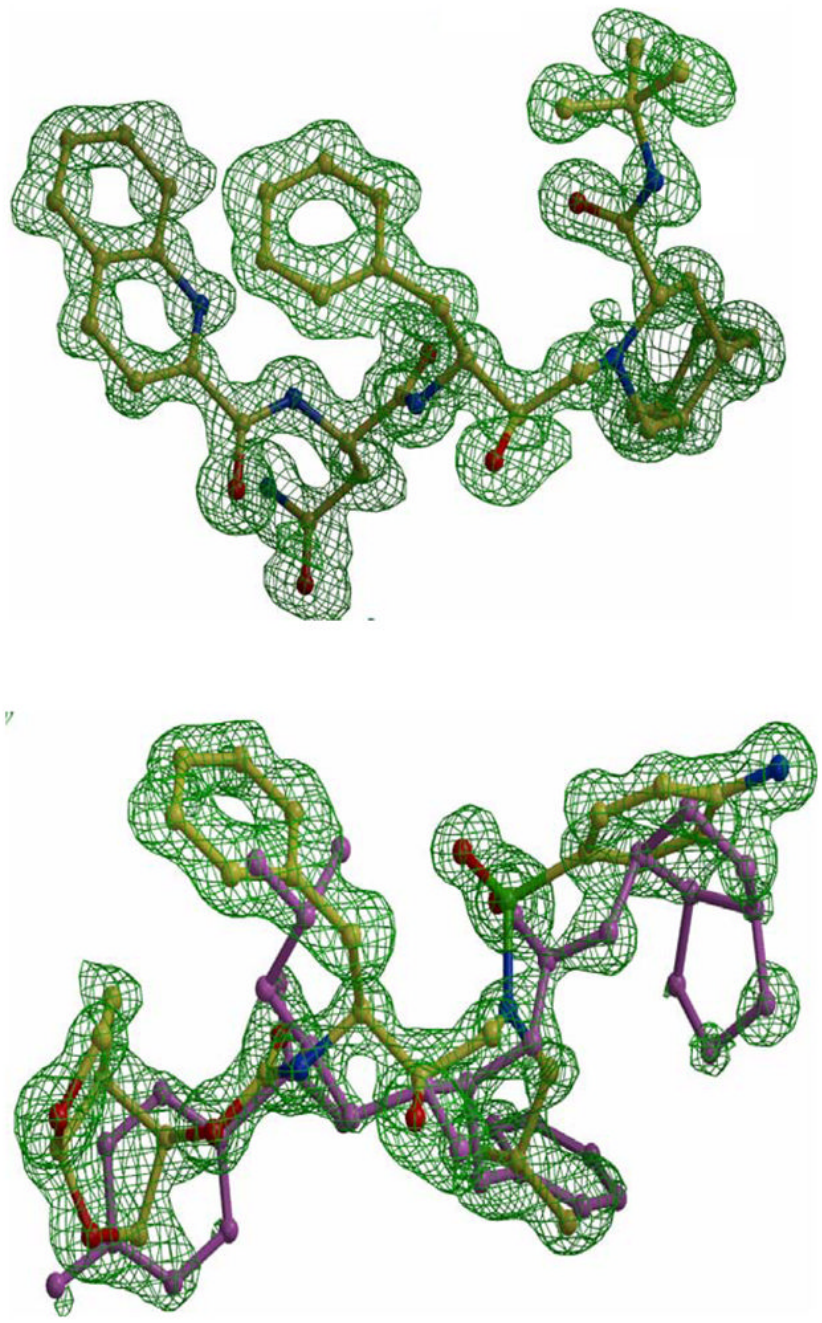

Figure 3.
The Fo-Fc omit maps of saquinavir (upper panel) and darunavir (lower panel) contoured at 3.3 sigma. Saquinavir is colored by atom type from complex PR_{I54V}-SQV. Darunavir is from complex PR_{I54V}-DRV showing alternate conformations of 60/40% occupancy. The major conformation is colored by atom type and the minor is colored pink.

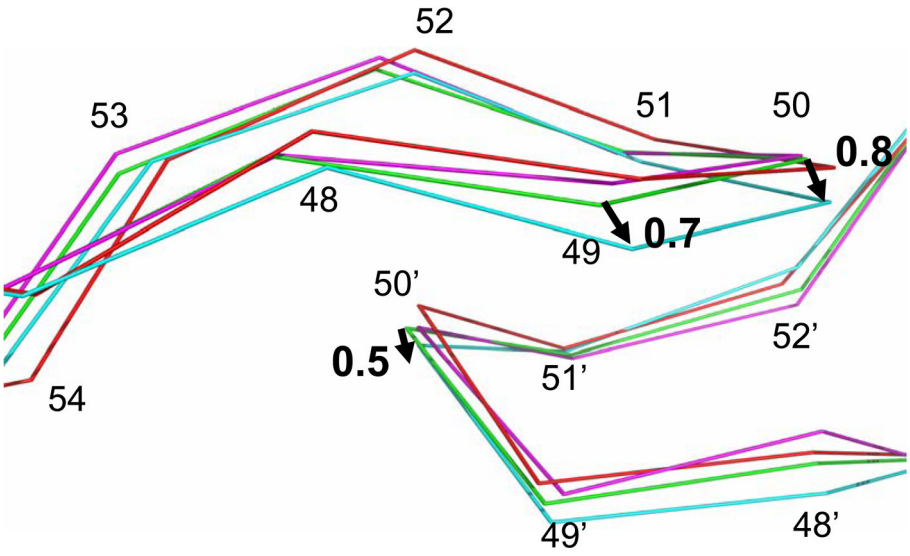

Figure 4.

The flap regions for superimposed complexes with darunavir. The wild type PR is in green, PR_{G48V} in cyan, PR_{I54V} in magenta and PR_{I54M} in red. The arrows indicate the shifts between Cα atoms of PR_{G48V} and of the wild type PR with distances in Å.

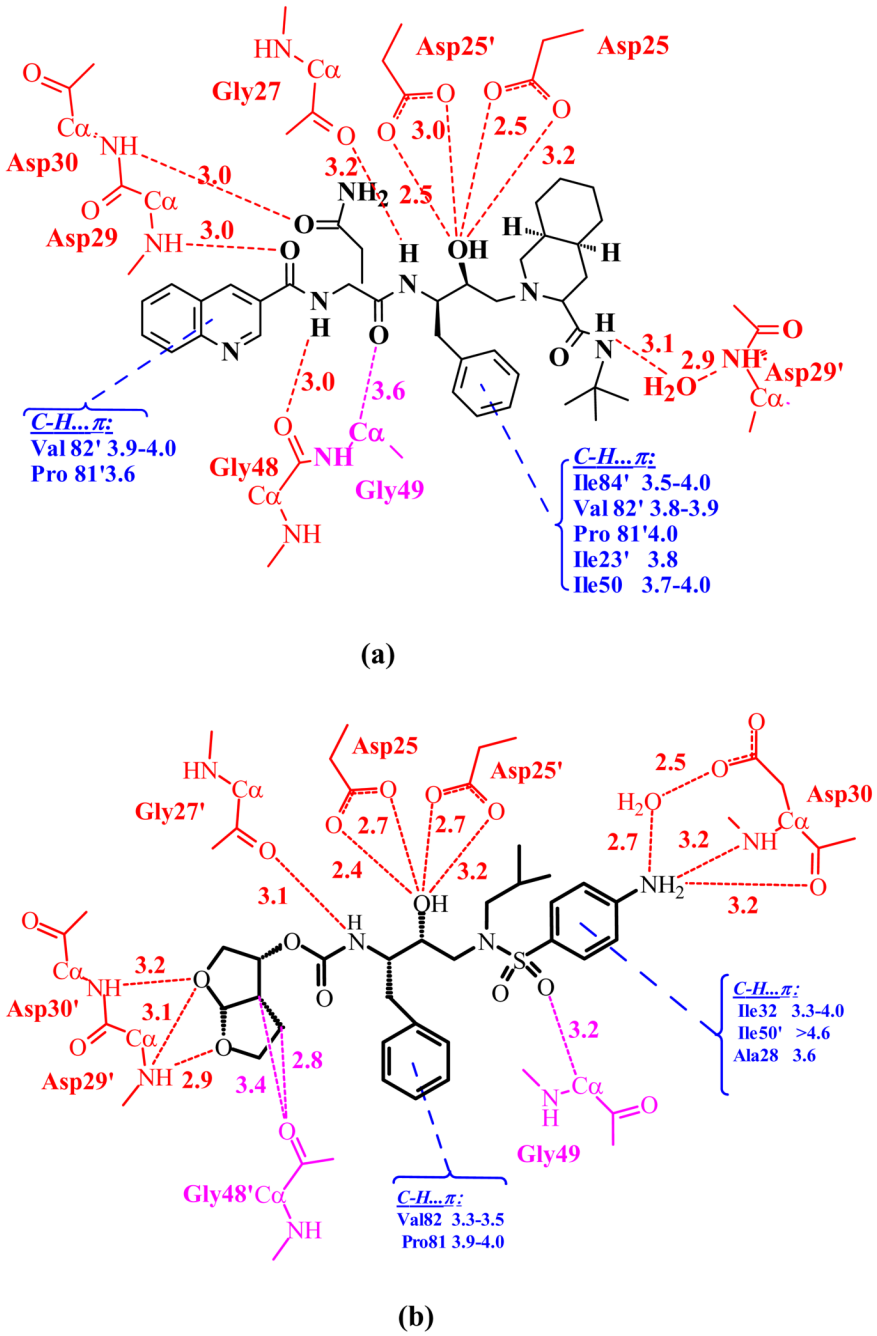

Figure 5.

PR_{I54M} interactions with inhibitor. (a) The major orientation of saquinavir. (b) The major orientation of darunavir. Hydrogen bonds are indicated in red, CH-π interactions in blue and C-H…O in purple. Interatomic distances are shown in Å. Note that the water-mediated interaction of the NH2 of darunavir with the Asp30 side chain is replaced by a direct hydrogen bond in the wild type PR and the other mutant structures.

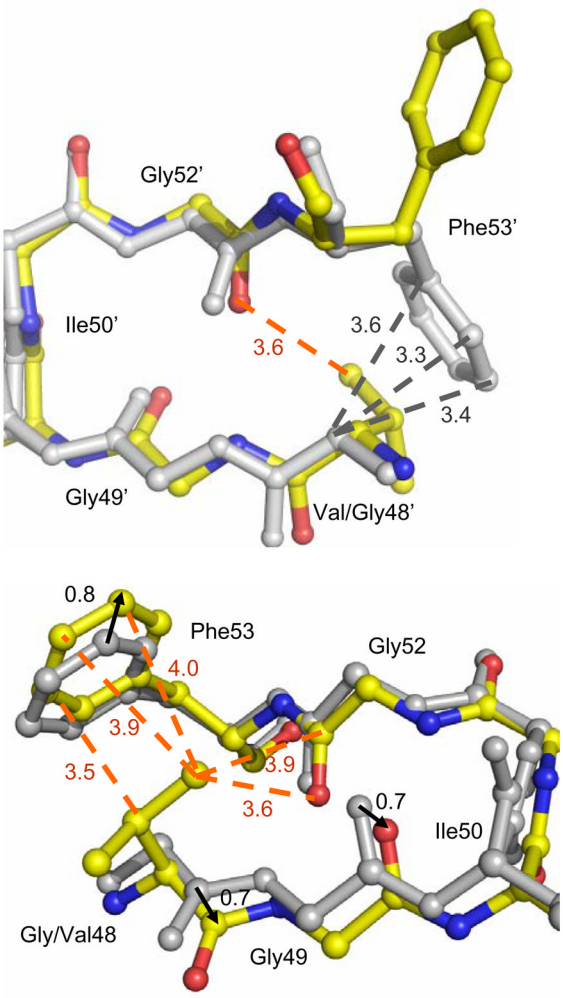

(a)

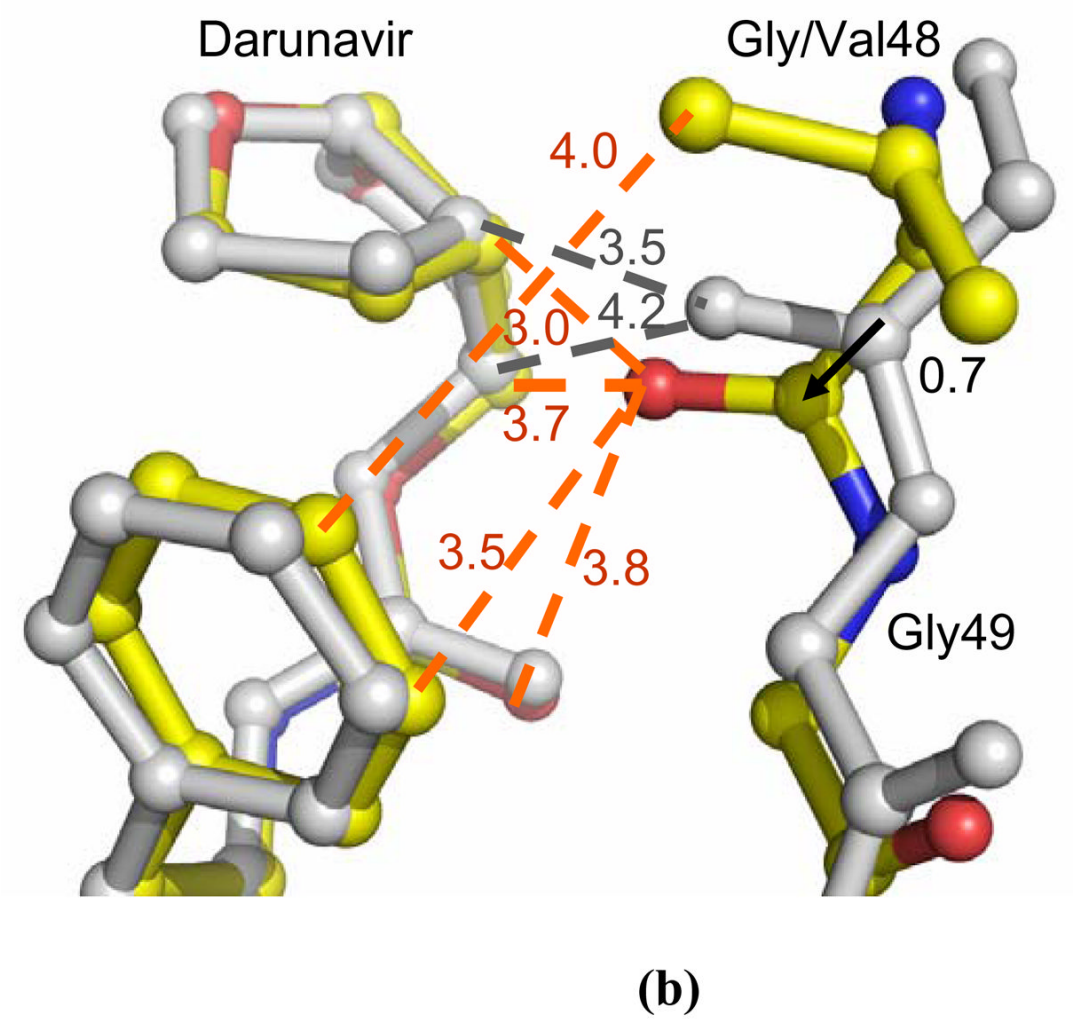

Figure 6.

(a) Comparison of the flaps of PR_{G48V}-DRV and of wild type PR-DRV in the two subunits. (b) Selected PR_{G48V} interactions with darunavir in the minor conformation. The mutant structures are colored by atom type and wild type PR is in grey. Dashed lines indicate van der Waals interactions with interatomic distances shown in Å. The arrows show the shift between the two structures with distances in Å.

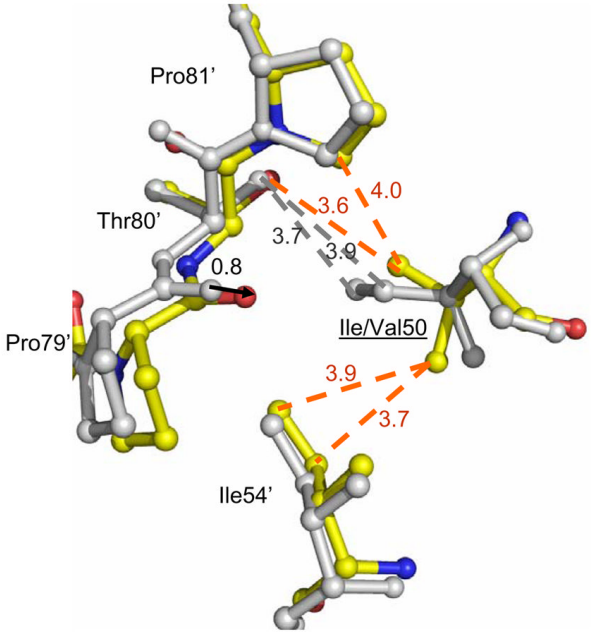

(a)

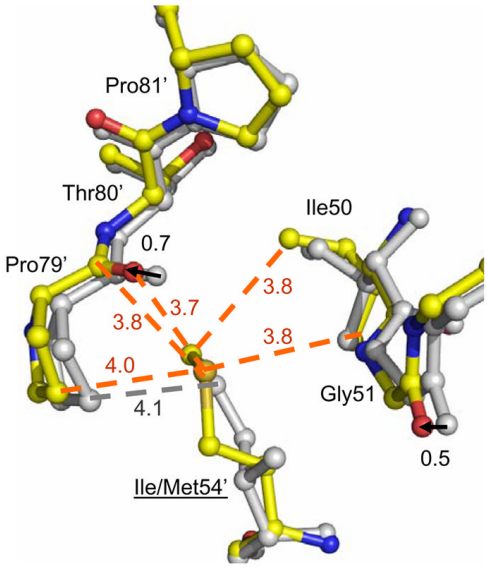

(b)

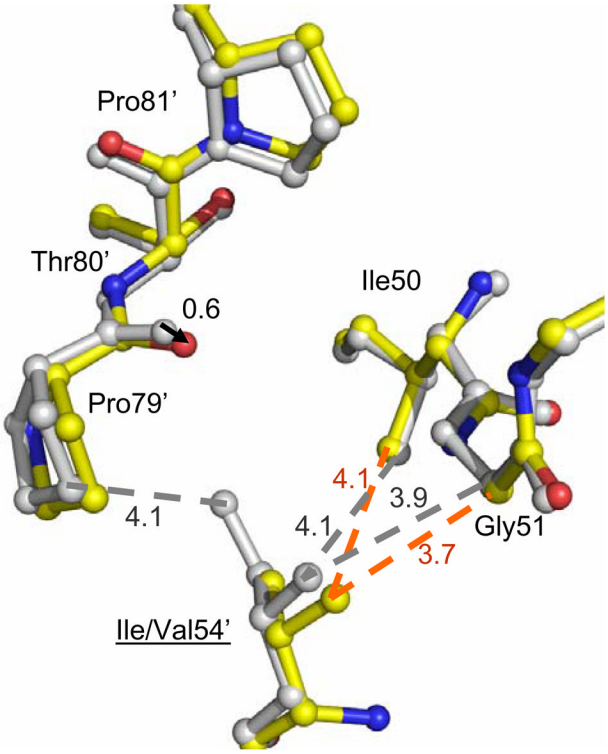

Figure 7.

The interactions of residues 50, 51, 54 and 79–81 in (a) PR_{I50V}-SQV, (b) PR_{I54M}-DRV, and (c) PR_{I54V}-DRV. The structures of mutants are colored by atom types and the corresponding structures of wild type PR are grey. Dashed lines indicate van der Waals interactions with interatomic distances shown in Å. The arrows show the shift between the two structures with distances in Å.

Table 1

Kinetic parameters for substrate hydrolysis and inhibition of darunavir and saquinavir.

Mutant	K_m (μM)	k_{cat} (/min)	k_{cat}/K_m (/min.μM)	Relative k_{cat}/K_m	K_i (nM)	Relative K_i	K_i (nM)	Relative K_i
					DRV		SQV	
PR	30±5	194±23	7.4±1.2	1.0	0.58±0.10	1	0.42±0.07	1
PR_{G48V}	91±8	220±9	2.4±0.2	0.3	17±2	29	36±3	86
PR_{I50V}	109±4	68±2	0.62±0.02	0.1	18±1	31	10±1	24
PR_{I54V}	43±9	134±28	3.1±0.7	0.4	5±1	8	6±1	15
PR_{I54M}	41±3	301±22	7.3±0.5	1.0	1.6±0.1	3	2.2±0.3	5

Table 2

Crystallographic Data Collection and Refinement Statistics

Protease Mutant		**PR_{I50V}**	**PR_{I54V}**	**PR_{I54M}**	**PR_{G48V}**	**PR_{I54V}**	**PR_{I54M}**
Inhibitors		**SQV**	**SQV**	**SQV**	**DRV**	**DRV**	**DRV**
Space group		$P2_12_12$	$P2_12_12$	$P2_12_12$	$P2_12_12$	$P2_12_12$	$P2_12_12$
Unit cell dimensions (Å)	a	58.9	58.7	59.5	58.2	58.8	58.6
	b	86.0	85.9	85.7	86.2	86.1	85.7
	c	46.4	46.38	46.2	45.9	46.2	46.0
Unique reflections		69158	101144	103172	40435	100265	53524
R_{merge} (%) Overall (final shell)		8.9 (53.7)	10.0 (42.3)	8.8 (25.8)	9.4 (20.3)	10.8 (41.7)	8.9 (57.6)
I/sigma(I) Overall (final shell)		13.5 (1.8)	16.8 (2.5)	21.9 (7.0)	13.2 (3.0)	17.8 (1.8)	24.4 (2.2)
Resolution range for refinement (Å)		10–**1.20**	10–**1.05**	10–**1.05**	10–**1.40**	10–**1.05**	10–**1.30**
R_{work} (%)		15.0	15.0	11.9	16.0	15.9	15.1
R_{free} (%)		19.2	17.4	14.7	22.7	17.96	19.5
No. of waters		200	223	209	174	212	161
Completeness (%) Overall (final shell)		93.1 (79.4)	92.5 (58.1)	93.4 (79.3)	87.5 (55.8)	91.2 (58.7)	94.4 (80.8)
RMS deviation from ideality							
Bonds (Å)		0.014	0.017	0.017	0.011	0.017	0.013
Angle distance (Å)		0.032	0.033	0.036	0.029	0.037	0.034
Average B-factors ($Å^2$)							
Main chain		10.2	14.0	10.1	15.7	15.5	16.9
Side chain		18.7	19.9	19.1	25.8	21.4	26.4
Inhibitor		9.4	17.0	10.8	13.8	12.8	16.8
Solvent		26.1	33.5	26.0	29.8	32.0	19.0
Inhibitor occupancy (%)		80/20	100	75/25	60/40	60/40	70/30